Semicond. Sci. Technol. **26** (2011) 014037 (8pp) doi:10.1088/0268-1242/26/1/014037

Band parameters and strain effects in ZnO and group-III nitrides

Qimin Yan[1], Patrick Rinke[1,2], M Winkelnkemper[3], A Qteish[4], D Bimberg[3], Matthias Scheffler[1,2] and Chris G Van de Walle[1]

[1] Materials Department, University of California, Santa Barbara, CA 93106-5050, USA
[2] Fritz-Haber-Institut der Max-Planck-Gesellschaft, Faradayweg 4-6, D-14195 Berlin, Germany
[3] Institut für Festkörperphysik, Technische Universität Berlin, Hardenbergstraße 36, D-10623 Berlin, Germany
[4] Department of Physics, Yarmouk University, 21163-Irbid, Jordan

E-mail: qimin@engineering.ucsb.edu

Received 7 June 2010, in final form 21 July 2010
Published 15 December 2010
Online at stacks.iop.org/SST/26/014037

Abstract
We present consistent sets of band parameters (including band gaps, crystal-field splittings, effective masses, Luttinger and E_P parameters) for AlN, GaN, InN and ZnO in the wurtzite phase. For band-energy differences we observe a pronounced nonlinear dependence on strain. Consistent and complete sets of deformation potentials are then derived for realistic strain conditions in the linear regime around the experimental equilibrium volume. To overcome the limitations of density-functional theory in the local-density and generalized-gradient approximations we employ the Heyd–Scuseria–Ernzerhof hybrid functional as well as exact exchange (OEPx)-based quasi-particle energy calculations in the G_0W_0 approach.

(Some figures in this article are in colour only in the electronic version)

1. Introduction

The field of lighting and general illumination is currently experiencing a transition from incandescent and fluorescent to solid-state light sources. The materials class that is driving this shift is the group-III nitrides [1]. Nitride-based light-emitting diodes (LEDs) [2, 3] are currently the only commercially available solution for the violet to green part of the optical spectrum, and the market for LEDs and laser diodes (LDs) has grown extensively in the last few years. Nitride-based LDs in violet are widely used in optical storage media, and other optoelectronic applications [4–6] are being explored.

Triggered by the success of the nitrides, research into ZnO has been experiencing a renaissance in the last few years [7] due to its similarity with GaN. ZnO is a promising candidate for optoelectronic applications such as transparent electrodes in electronic circuits [8], solar cells [9] or transparent thin-film transistors [10], and ZnO-based hybrid organic–inorganic interfaces are now being explored [11, 12] as novel optoelectronic devices. ZnO-based heterostructures have also received increased attention, since the successful growth of $Zn_{1-x}Mg_xO$ and $Zn_{1-x}Cd_xO$ alloys with low Mg/Cd concentration has been demonstrated [13–19]. The fact that the quantum Hall effect has been observed in an oxide system [20] demonstrates the quality that $ZnO/Zn_{1-x}Mg_xO$ interfaces have now reached and confirms that oxide electronics is an emerging field [7, 21].

For future progress in these directions, reliable materials parameters beyond the fundamental band gap are needed to aid the interpretation of experimental observations and to enable reliable simulations of (hetero-)structures [22–27]. These include effective masses, valence-band (Luttinger or Luttinger-like) parameters and strain deformation potentials. Ideally, the parameters are determined experimentally. However, for ZnO and the group-III nitrides many of the key band and strain parameters have not been conclusively determined until now, despite the extensive research effort in this field [28–30].

Materials parameters can be derived from first-principles electronic-structure methods for bulk phases, but the size and complexity of structures required for device simulations currently exceed the capabilities of first-principles electronic-structure tools. To bridge this gap first-principles calculations can be used to parametrize simplified methods, such as the $\mathbf{k}\cdot\mathbf{p}$ method [31–34], the tight-binding (TB) method [35–39]

or the empirical pseudo-potential method (EPM) [40], which are applicable to large-scale heterostructures at reasonable computational expense.

In this paper we demonstrate that state-of-the-art first principles methods in combination with the $\mathbf{k}\cdot\mathbf{p}$ approach can be used to derive consistent sets of materials parameters for the group-III nitrides and ZnO. We present a complete set of band dispersion parameters (effective masses and Luttinger parameters) and deformation potentials ($a_{cz}-D_1$, $a_{ct}-D_2$, D_3, D_4, D_5 and D_6) for wurtzite AlN, GaN, InN and ZnO. The strain dependence was computed with density-functional theory (DFT). To ameliorate the band-gap problem of the widely applied local-density and generalized-gradient approximations (LDA and GGA, respectively) we use the Heyd–Scuseria–Ernzerhof (HSE) [41, 42] hybrid functional. Furthermore, quasiparticle band structures were calculated with many-body perturbation theory (MBPT) in the G_0W_0 approximation [43] based on DFT calculations in the exact-exchange optimized effective potential (OEPx) approach [44] and including LDA correlation G_0W_0@OEPx(cLDA) [45, 46]. We show that the G_0W_0@OEPx(cLDA) band structure of ZnO is in excellent agreement with recent angle-resolved photoemssion spectroscopy (ARPES) data. The comparison illustrates clearly, however, that despite the steadily increasing resolution, ARPES measurements are not yet suitable for determining band parameters without the aid of first-principles calculations.

The band parameters and deformation potentials $a_{cz}-D_1$, $a_{ct}-D_2, D_3, D_4, D_5$ for the nitrides were previously presented in [23] and [47]. Here we add the deformation potential D_6 and results for ZnO. We also put the nitride deformation potentials into the context of recent experimental studies that were not available at the time of our earlier work. The paper is structured as follows: in section 2 we briefly review our computational approach, and in section 3 we present and discuss our results before we conclude in section 4.

2. Computational approach

2.1. Quasiparticle band structures and band parameters

The band structure of a solid is given by the momentum-resolved ionization energies (holes) and electron affinities (electrons) as measured in direct and inverse photoemission spectroscopy. In theoretical spectroscopy MBPT provides a rigorous and systematic quantum mechanical framework to describe the spectral properties of a system. Within MBPT Hedin's GW approach [43] is currently the state-of-the-art in theoretical spectroscopy for band structures of solids. Here we apply GW as single post-correction (G_0W_0) to a ground-state calculation in DFT.

For most of the early days of GW calculations in solids, LDA and GGA were almost exclusively used as the starting point for G_0W_0 [48–50], because more advanced functionals were not widely available [51]. Ground-state functionals that are self-interaction (SI) free (such as OEPx [44]) or significantly reduce the SI error have proven to be particularly advantageous—if not necessary—for materials with d- and f-electrons [46, 52–54]. For the compounds considered in this paper this becomes most apparent for the band gap, which is severely underestimated by the Kohn–Sham eigenvalue difference in LDA and GGA. For ZnO this underestimation is particularly severe: LDA gives 0.7 eV at the experimental lattice constant, much smaller than the experimental 3.4 eV gap, while for InN it even results in an overlap between the conduction and the valence bands and thus an effectively metallic state [23, 55]. It goes without saying that a $\mathbf{k}\cdot\mathbf{p}$ parametrization derived from such an LDA band structure would not appropriately reflect the properties of bulk InN.

Here we apply the G_0W_0 approach to DFT calculations in the OEPx(cLDA) approach. Unlike in LDA and GGA the SI error in OEPx(cLDA) is greatly reduced (OEPx is fully SI free) and correctly predicts InN to be semiconducting with the right band ordering in the wurtzite phase [56, 57]. Combining OEPx(cLDA) with G_0W_0 [G_0W_0@OEPx(cLDA)] yields band gaps for II–VI compounds, Ge, ScN and group-III nitrides that agree to better than 0.3 eV with experiment [23, 45, 46, 57, 58], which can also be seen in table 1 for the four compounds considered in this paper. This is currently the best accuracy one can expect from a state-of-the-art first principles theory that does not rely on fitting parameters, as the empirical pseudopotential or tight-binding methods do. To be free of fitting parameters is essential for a predictive theory as the example of InN illustrates, whose band gap was believed to be ∼1.9 eV until the year 2002, when it was revised to a much lower value of ∼0.7 eV [59–63]. Improving the accuracy of band-gap calculations in MBPT by, for example, including the electron–phonon coupling [64–67] or higher order correlation effects through vertex corrections [68–72] is currently an active field of research.

We would like to emphasize that energy differences that do not involve a difference between electron and hole states are given more accurately, as figure 1 shows and the example of effective masses demonstrates (see e.g. [23, 73]). With regard to crystal-field splittings, the comparison between theory

Table 1. Equilibrium lattice parameters (a, c and u) obtained with the HSE method and band gaps (E_g) and crystal-field splitting Δ_{cr} obtained with HSE and G_0W_0@OEPx(cLDA) (abbreviated here by G_0W_0). The G_0W_0 results are obtained at experimental lattice parameters. Experimental lattice parameters at $T = 300$ K and band-gap values are taken from [22], [23], [85] and [86].

	Method	a (Å)	c (Å)	u	E_g (eV)	Δ_{cr} (meV)
AlN	HSE	3.102	4.971	0.3819	5.64	−236
	G_0W_0	–	–	–	6.47	−295
	Exp.	3.112	4.982	–	6.25	−230
GaN	HSE	3.182	5.173	0.3772	3.24	19
	G_0W_0	–	–	–	3.24	34
	Exp.	3.190	5.189	–	3.51	9–38
InN	HSE	3.548	5.751	0.3796	0.68	37
	G_0W_0	–	–	–	0.69	66
	Exp.	3.540	5.706	–	0.65	19–24
ZnO	HSE	3.264	5.238	0.3807	2.48	66
	G_0W_0	–	–	–	3.22	74
	Exp.	3.249	5.205	–	3.43	43

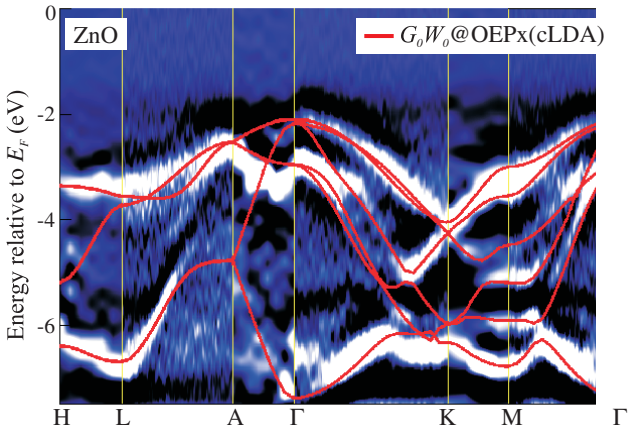

Figure 1. ARPES data for the upper valence bands of ZnO [82, 83] with the G_0W_0@OEPx(cLDA) band structure superimposed (red lines).

and experiment is aggravated by the spread in the reported experimental values and the fact that the separation between exciton lines measures the combined effect of the crystal-field and the spin–orbit splitting. For InN there is an additional question mark on the reliability of the experimental values. Due to the intrinsic n-type conductivity of all InN samples, the crystal-field splitting has only been inferred indirectly so far, because the exciton structure is masked by the free carriers in the conduction band.

The OEPx calculations in the present work were performed with the pseudopotential plane-wave code `S/PHI/nX` [74], while for the G_0W_0 calculations we have employed the G_0W_0 spacetime method [75] in the `gwst` implementation [76–78]. Local LDA correlation is added in all OEPx calculations. Here we use the parametrization of Perdew and Zunger [79] for the correlation energy density of the homogeneous electron gas based on the data of Ceperley and Alder [80]. Consistent OEPx(cLDA) pseudopotentials were used throughout [81]. The cation *d* electrons were included explicitly [45, 56]. For ZnO we use a plane-wave cutoff of 75 Ry and include empty states up to 55 Ry (∼2000 bands at every *k*-point) in the polarizability in both OEPx(cLDA) and G_0W_0@OEPx(cLDA). All calculations were performed at the experimental lattice constants, except for ZnO, where we took the HSE lattice constants (see also table 1). For additional technical details and convergence parameters we refer to previous work [45, 57].

Figure 1 shows ARPES data for the upper valence bands of ZnO [82, 83]. The G_0W_0@OEPx(cLDA) band structure (superimposed in red) is in excellent agreement with the ARPES data both in terms of the band energies and band curvatures. However, figure 1 also illustrates that experimental band structures [82, 84] are not yet accurate enough to determine band parameters such as effective masses or crystal-field splittings without first-principles calculations.

In this work we have extracted the band gaps and the crystal-field splittings directly from the respective G_0W_0@OEPx(cLDA) band structures. Effective masses, on the other hand, were determined by fitting the Luttinger parameters A_i, and E_P values of the 8 × 8 strain free $\mathbf{k}\cdot\mathbf{p}$ Hamiltonian given by Bir and Pikus [87] to the G_0W_0@OEPx(cLDA) band structures in the vicinity of Γ-point [23]. The relevant computational details and formulas are given in [23].

2.2. DFT-HSE and strain

In the exploration of the strain dependence in wurtzite crystals the internal coordinate u needs to be relaxed for every new strain condition. This requires the computation of forces (or at least total energies), which is currently not feasible in the GW approach. For this reason we use the HSE [41, 42] hybrid DFT functional as implemented in the VASP code [88]. HSE incorporates 25% of exact, non-local exchange that is screened at long distances. The screening parameter μ in HSE was fixed at a value of 0.2 (HSE06). Table 1 illustrates that HSE produces band gaps in much better agreement with experiment than DFT in the LDA or GGA. The remaining difference to the experimental band gaps has only a small effect on the computed strain deformation potentials. We verified this by increasing the factor that controls the admixture of exact exchange until the experimental band gaps were reproduced by HSE. The calculated deformation potentials change by only a few per cent [89], a difference much smaller than the experimental error bars reported in table 4.

HSE also provides a good description of the structural properties of the nitrides [47]. The calculations were carried out in the projector augmented wave (PAW) method using a plane-wave cutoff of 600 eV to determine the internal displacement parameter u accurately. The Brillouin zone was sampled with a 6 × 6 × 4 Γ-centered *k*-point mesh. Throughout, the internal displacement parameter u is fully relaxed. Table 1 shows that the HSE method gives lattice parameters for AlN, GaN, InN and ZnO within 1% of the experimental values.

The strain dependence of the optical transition energies can then be computed directly by monitoring the HSE eigenvalue differences as a function of strain. Deformation potentials are obtained in a similar way. Diagonalizing the strained 6 × 6 $\mathbf{k}\cdot\mathbf{p}$ Hamiltonian for the valence bands of wurtzite semiconductors [87] gives analytic expressions for the three highest valence-to-conduction-band transitions (E_A, E_B and E_C) in terms of strain deformation potentials.

Four different types of strain may be present in binary wurtzite systems: biaxial strain in the *c*-plane ($\varepsilon_{xx} = \varepsilon_{yy}$, $\varepsilon_\perp = \varepsilon_{xx} + \varepsilon_{yy}$), uniaxial strain along the *c*-axis (ε_{zz}), anisotropic strain in the *c*-plane ($|\varepsilon_{xx} - \varepsilon_{yy}|$) and shear strain ($\varepsilon_{xz}$ and ε_{yz}). Biaxial strain in the *c*-plane and uniaxial strain out of the *c*-plane change the transition energies in a similar way:

$$\begin{aligned} E_{A/B} &= E_{A/B}(0) + (a_{cz} - D_1)\varepsilon_{zz} + (a_{ct} - D_2)\varepsilon_\perp \\ &\quad - (D_3\varepsilon_{zz} + D_4\varepsilon_\perp), \\ E_C &= E_C(0) + (a_{cz} - D_1)\varepsilon_{zz} + (a_{ct} - D_2)\varepsilon_\perp. \end{aligned} \quad (1)$$

Note that a_{cz} (a_{ct}) are conduction-band deformation potentials that are combined with the valence-band deformation

Table 2. Luttinger parameters and transition matrix elements E_P for AlN, GaN, InN and ZnO obtained by fitting the $\mathbf{k}\cdot\mathbf{p}$ Hamiltonian to the respective G_0W_0@OEPx(cLDA) band structures.

Parameter	AlN	GaN	InN	ZnO
A_1	−3.991	−5.947	−15.803	−2.743
A_2	−0.311	−0.528	−0.497	−0.393
A_3	3.671	5.414	15.251	2.377
A_4	−1.147	−2.512	−7.151	−2.069
A_5	−1.329	−2.510	−7.060	−2.051
A_6	−1.952	−3.202	−10.078	−2.099
A_7 (eVÅ)	0.026	0.046	0.175	0.001
$m_e^{\parallel}$	0.322	0.186	0.065	0.246
$m_e^{\perp}$	0.329	0.209	0.068	0.329
$E_P^{\parallel}$ (eV)	16.97	17.29	8.74	13.042
$E_P^{\perp}$ (eV)	18.17	16.27	8.81	9.604

potentials D_1 (D_2) to describe the dependence of band gaps on strain.

Anisotropic strain in the c-plane ($|\varepsilon_{xx} - \varepsilon_{yy}| \neq 0$) lowers the crystal symmetry from C_{6v} to C_{2v}. This lifts the degeneracy of the Γ_6 state and leads to a splitting between the heavy-hole (HH) and light-hole (LH) bands, which can be expressed in terms of the deformation potential D_5 as follows:

$$\Delta E = |E_{HH} - E_{LH}| = 2|D_5(\varepsilon_{xx} - \varepsilon_{yy})|. \tag{2}$$

A special strain component that is often not considered is shear strain (ε_{xz} and ε_{yz}). The effect of shear strain on the band structure of wurtzite materials is given by the deformation potential D_6. The crystal-field split-off (CH) band energy for the unstrained system is set as zero and the topmost three valence band energies are

$$E_1 = \Delta_{\mathrm{cr}},$$
$$E_{2,3} = \frac{\Delta_{\mathrm{cr}}}{2} \pm \frac{\sqrt{\Delta_{\mathrm{cr}}^2 + 8D_6^2\varepsilon_{xz}^2}}{2}. \tag{3}$$

These various expressions can now be fitted to HSE calculations for different strain conditions to determine the deformation potentials. Details of the procedure can be found in [47].

3. Results

3.1. Band parameters

Table 2 lists the Luttinger parameters and transition matrix elements E_P for AlN, GaN, InN and ZnO obtained by fitting the $\mathbf{k}\cdot\mathbf{p}$ Hamiltonian to the respective G_0W_0@OEPx(cLDA) band structures. We have previously demonstrated that for the nitrides the effective masses derived from these $\mathbf{k}\cdot\mathbf{p}$ parameters are in good agreement with currently available experimental values [23]. For ZnO they agree well with the effective masses obtained from the G_0W_0@HSE calculations by Schleife *et al* [73].

As one would expect, the Luttinger and E_p parameters of ZnO are similar to those of GaN. Two differences are noteworthy, however. First, the absolute value of A_1 and A_3 is twice as large in GaN than in ZnO, which is a direct result of the smaller in-plane heavy hole effective mass in GaN $\left(m_{\mathrm{HH}}^{\parallel}(\mathrm{GaN}) = 1.88 \text{ versus } m_{\mathrm{HH}}^{\parallel}(\mathrm{ZnO}) = 2.73\right)$. Second, unlike in the nitrides the E_P parameters in ZnO are highly anisotropic. This is reflected in the anisotropy of the conduction-band effective masses which is much more pronounced in ZnO than in the nitrides.

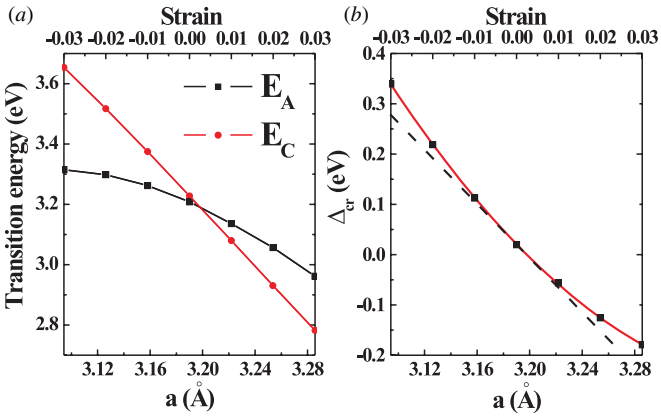

Figure 2. (*a*) Transition energies E_A and E_C of GaN under biaxial stress. (*b*) Crystal-field splitting of GaN under biaxial stress. Symbols: HSE data; lines: quadratic fits.

3.2. Strain dependence

In this section we present results for two types of realistic strain conditions: biaxial stress and hydrostatic pressure. Epitaxial nitride layers often experience biaxial stress induced by pseudomorphic growth. Under such stress, the compressive biaxial strain in the c-plane is accompanied by a tensile out-of-plane uniaxial strain:

$$\varepsilon_{zz} = -2\frac{C_{13}}{C_{33}}\varepsilon_{xx}, \qquad \varepsilon_{xx} = \varepsilon_{yy} \neq 0. \tag{4}$$

Here we use the elastic constants obtained from the theoretical calculations of Wright *et al* [90]. Figure 2 shows the transition energies between the first conduction band and the topmost three valence bands (HH, LH and CH) of GaN under biaxial stress in the c-plane for the strain range ±3%. Interestingly, we observe a pronounced nonlinear behavior in the transition energy between the CB and the HH/LH bands, and also in the crystal-field splitting (the difference between HH/LH and CH bands). Both nonlinearities can be well described by a quadratic dependence as demonstrated by the fitted curves. This implies that the slope (needed to determine the deformation potentials) differs for different lattice parameters. Similar nonlinearities are observed for AlN and InN under biaxial stress (not shown here) and for ZnO (see figure 3). For systems with large internal strain components, such as InGaN alloys grown on GaN substrates, these nonlinearities should be taken into account.

Another realistic strain condition could be induced by hydrostatic pressure, where the stress components along three directions are the same, $\sigma_{xx} = \sigma_{yy} = \sigma_{zz}$. The in-plane strain

Table 3. Deformation potentials (in eV) of AlN, GaN, InN and ZnO obtained by the HSE method. For GaN cross-checks with G_0W_0@OEPx(cLDA) are also listed.

	Method	$a_{cz} - D_1$	$a_{ct} - D_2$	D_3	D_4	D_5	D_6
AlN	HSE	−4.21	−12.07	9.22	−3.74	−3.30	−4.49
GaN	HSE	−5.81	−8.92	5.45	−2.97	−2.87	−3.95
	G_0W_0	−5.33	−8.84	5.80	−3.09	–	–
InN	HSE	−3.64	−4.58	2.68	−1.78	−2.07	−3.02
ZnO	HSE	−3.06	−2.46	0.47	−0.84	−1.21	−1.77

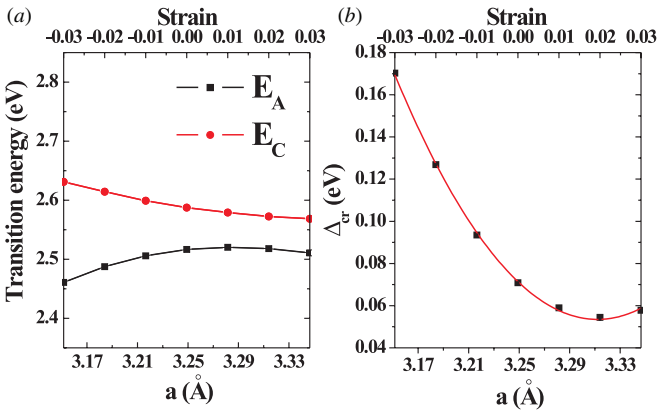

Figure 3. (*a*) Transition energies E_A and E_C of ZnO under biaxial stress. (*b*) Crystal-field splitting of ZnO under biaxial stress. Symbols: HSE data; lines: quadratic fits.

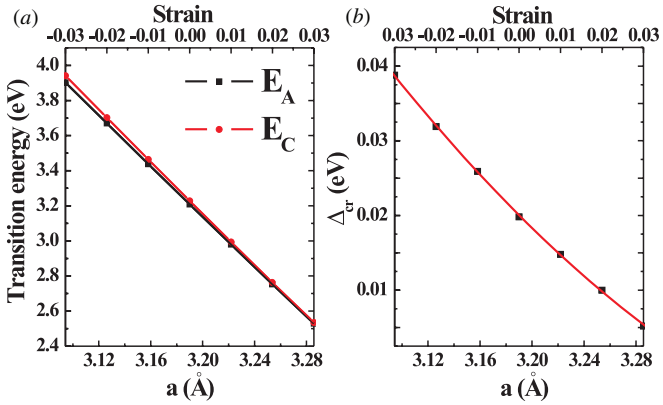

Figure 4. Same as figure 2 but for hydrostatic pressure.

and out-of-plane strain now have the same sign but the strain components are not isotropic:

$$\varepsilon_{zz} = \frac{C_{11} + C_{12} - 2C_{13}}{C_{33} - C_{13}}\varepsilon_{xx},$$
$$\varepsilon_{xx} = \varepsilon_{yy} = \frac{C_{33} - C_{13}}{C_{33}(C_{11} + C_{12}) - 2C_{13}^2}\sigma_{zz}. \quad (5)$$

Under hydrostatic pressure conditions, as shown in figure 4(*a*), the transition energies change almost linearly over the strain range ±3%. The strain nonlinearity is therefore much weaker when hydrostatic strain is applied to wurtzite semiconductors.

To determine the strain deformation potentials we calculate the dependence of the change in transition energies by computing the band structure in HSE for the four different strain conditions given in equations (1)–(3). From the slopes of the transition energies under biaxial or uniaxial strain, the deformation potentials $a_{cz} - D_1$, $a_{ct} - D_2$, D_3 and D_4 can be obtained. Anisotropic strain in the *c*-plane yields D_5 and shear strain yields D_6. By constraining the strain range to realistic strain conditions in the linear regime around the experimental lattice parameters (or theoretical lattice parameters for ZnO)[5], we derive a consistent and complete set of deformation potentials for AlN, GaN, InN and ZnO from HSE calculations, as listed in table 3.

[5] For ZnO we chose the theoretical lattice constants for consistency with calculations performed for MgO and CdO, which crystallize in the rocksalt phase. Experimental lattice parameters for MgO and CdO are currently not available.

With the exception of $a_{cz} - D_1$ the deformation potentials increase in magnitude from InN to GaN to AlN. In contrast to the band parameters, the deformation potentials for ZnO differ appreciably from those of GaN. They are in fact closer to, and even smaller in magnitude than, those for InN. This indicates that the response of the electronic structure to external strain perturbations is correlated not only with the band gaps, but also with other physical and chemical properties such as bonding strength.

To cross-check our HSE calculations, in particular for the band-gap-related deformation potentials $a_{cz} - D_1$ and $a_{ct} - D_2$, we performed G_0W_0@OEPx(cLDA) calculations for GaN. As seen in table 3, both deformation potential sets are in good agreement, validating the consistency of the two approaches for band-structure-derived properties such as deformation potentials. We also performed LDA and GGA–PBE calculations (not shown here). In comparison with HSE, LDA and PBE underestimate the magnitude of the band-gap-related deformation potentials $a_{cz} - D_1$ and $a_{ct} - D_2$, but give similar results for the other deformation potentials. A full comparison between HSE, LDA and PBE will be published elsewhere.

A comparison to the available experimental deformation potentials is presented in table 4. Our deformation potentials fall within the experimentally reported range, but this range of reported experimental values is very wide for GaN. Our values are in reasonable agreement with those reported in [97] (last line for GaN in table 4). A similar level of agreement is achieved for ZnO. Note that our sign convention for D_3 and D_4 is opposite to that in [99] and [100]; we have therefore

Table 4. Experimentally determined deformation potentials (eV) of wurtzite GaN, InN and ZnO.

	Method	$a_{cz} - D_1$	$a_{ct} - D_2$	D_3	D_4	D_5	D_6
GaN	HSE	−5.81	−8.92	5.45	−2.97	−2.87	−3.95
	Exp.[91]	–	–	8.82	−4.41	–	–
	Exp.[92]	−6.50	−11.80	5.30	−2.70	–	–
	Exp.[93]	–	–	6.80	−3.40	−3.30	–
	Exp.[94]	−5.32	−10.23	4.91	−2.45	–	–
	Exp.[95]	–	–	–	–	−3.60	–
	Exp.[96]	−9.60	−8.20	1.90	−1.00	–	–
	Exp.[97]	−6.50	−11.20	4.90	−5.00	−2.80	−3.10
InN	HSE	−3.64	−4.58	2.68	−1.78	−2.07	−3.02
	Exp.[98]	−7.66	−2.59	5.06	−2.53	–	–
ZnO	HSE	−3.06	−2.46	0.47	−0.84	−1.21	−1.77
	Exp. [99]	−3.80	−3.80	0.80	−1.40	−1.20	|1.0|
	Exp. [100]	−3.90	−4.13	1.15	−1.22	−1.53	−0.92

changed the sign of these experimental values in the table. Deformation potentials for InN have recently been measured for the first time by Gil *et al* [98]. However, the intrinsic *n*-type nature of InN and the large lattice mismatch (either with a sapphire substrate or with GaN epilayers) complicate an accurate experimental determination. The difference with our computed values is considerable and more work is required in the future to understand these discrepancies.

Our *ab initio* calculations also allow us to assess the quasicubic approximation. The quasicubic approximation is often made in experimental studies, because it eliminates the explicit dependence on three deformation potentials. In the quasicubic approximation, the deformation potentials are related as follows: $D_3 = -2D_4$, $D_1 + D_3 = D_2$ and $D_3 + 4D_5 = \sqrt{2}D_6$. We find that $D_3 + 2D_4$ is 1.43, −0.52, −0.88 and −1.21 for AlN, GaN, InN and ZnO respectively. Obviously the quasicubic approximation is not valid in these wurtzite semiconductors, as also recently observed in the experimental work of [97].

4. Conclusions

In conclusion, the band dispersion and strain dependence of AlN, GaN, InN and ZnO have been presented. We obtain consistent sets of band parameters and deformation potentials by applying the G_0W_0@OEPx(cLDA) approach and hybrid functional DFT calculations. These band parameters and deformation potentials are critical for accurate modeling of nitride- and oxide-based device structures.

Acknowledgments

This work was supported by the Solid State Lighting and Energy Center at the University of California, Santa Barbara, and by the NSF MRSEC Program (DMR05-20415). It made use of the CNSI Computing Facility (NSF grant no CHE-0321368) and TeraGrid computing resources (NSF grant no DMR070072N). PR acknowledges the support of the Deutsche Forschungsgemeinschaft, the UCSB-MPG Program for International Exchange in Materials Science and the NSF-IMI Program (grant no DMR04-09848). DB and MW appreciate the support of DFG in the frame of SFB 787.

References

[1] Pimputkar S, Speck J S, Denbaars S P and Nakamura S 2009 *Nat. Photonics* **3** 180
[2] Nakamura S 1998 *Science* **281** 956
[3] Taniyasu Y, Kasu M and Makimoto T 2006 *Nature* **441** 325
[4] Fasoi G 1996 *Science* **272** 1751
[5] Nakamura S *et al* 1998 *Appl. Phys. Lett.* **72** 211
[6] Tojyo T, Asano T, Takeya M, Hino T, Kijima S, Goto S, Uchida S and Ikeda M 2001 *Japan. J. Appl. Phys.* **40** 3206
[7] Janotti A and Van de Walle C G 2009 *Rep. Prog. Phys.* **72** 126501
[8] Hirata G, McKittrick J, Cheeks T, Siqueiros J, Diaz J, Contreras O and Lopez O 1996 *Thin Solid Films* **288** 29
[9] Ramanathan K *et al* 2003 *Prog. Photovolt., Res. Appl.* **11** 225
[10] Hossain F M, Nishii J, Takagi S, Ohtomo A, Fukumura T, Fujioka H, Ohno H, Koinuma H and Kawasaki M 2003 *J. Appl. Phys.* **94** 7768
[11] Blumstengel S, Sadofev S, Xu C, Puls J, Johnson R L, Glowatzki H, Koch N and Henneberger F 2008 *Phys. Rev.* B **77** 085323
[12] Blumstengel S, Sadofev S and Henneberger F 2008 *New J. Phys.* **10** 065010
[13] Sharma A K, Narayan J, Muth J F, Teng C W, Jin C, Kvit A, Kolbas R M and Holland O W 1999 *Appl. Phys. Lett.* **75** 3327
[14] Makino T, Chia C H, Tuan N T, Sun H D, Segawa Y, Kawasaki M, Ohtomo A, Tamura K and Koinuma H 2000 *Appl. Phys. Lett.* **77** 975
[15] Coli G and Bajaj K K 2001 *Appl. Phys. Lett.* **78** 2861
[16] Park W I, Yi G-C and Jang H M 2001 *Appl. Phys. Lett.* **79** 2022
[17] Choopun S, Vispute R D, Yang W, Sharma R P, Venkatesan T and Shen H 2002 *Appl. Phys. Lett.* **80** 1529
[18] Sadofev S, Blumstengel S, Cui J, Puls J, Rogaschewski S, Schäfer P, Sadofyev Y G and Henneberger F 2005 *Appl. Phys. Lett.* **87** 098903
[19] Sadofev S, Blumstengel S, Cui J, Puls J, Rogaschewski S, Schäfer P and Henneberger F 2006 *Appl. Phys. Lett.* **89** 201907

[20] Tsukazaki A, Ohtomo A, Kita T, Ohno Y, Ohno H and Kawasaki M 2007 *Science* **315** 1388
[21] Ramirez A P 2007 *Science* **315** 1377
[22] Vurgaftman I and Meyer J R 2003 *J. Appl. Phys.* **94** 3675
[23] Rinke P, Winkelnkemper M, Qteish A, Bimberg D, Neugebauer J and Scheffler M 2008 *Phys. Rev.* B **77** 075202
[24] Park S-H, Kim K J, Yi S N, Ahn D and Lee S J 2005 *J. Korean Phys. Soc.* **47** 448
[25] Fan W, Abiyasa A, Tan S, Yu S, Sun X, Xia J, Yeo Y, Li M and Chong T 2006 *J. Cryst. Growth* **287** 28
[26] Abiyasa A P, Yu S F, Fan W J and Lau S P 2006 *IEEE J. Quantum Electron.* **42** 455
[27] Rozale H, Bouhafs B and Ruterana P 2007 *Superlattices Microstruct.* **42** 165
[28] Walukiewicz W, Ager J W III, Yu K M, Lilienthal-Weber Z, Wu J, Li S X, Jones R E and Denlinger J D 2006 *J. Phys. D: Appl. Phys.* **39** R83
[29] Vurgaftman I and Meyer J R 2003 *J. Appl. Phys.* **94** 3675
[30] Klingshirn C 2007 *Phys. Status Solidi* B **244** 3019
[31] Kane E O 1982 *Band Theory and Transport Properties* (*Handbook on Semiconductors* vol 1) ed W Paul (Amsterdam: North-Holland) p 195
[32] Andreev A D and O'Reilly E P 2000 *Phys. Rev.* B **62** 15851
[33] Fonoberov V A and Balandin A A 2003 *J. Appl. Phys.* **94** 7178
[34] Winkelnkemper M, Schliwa A and Bimberg D 2006 *Phys. Rev.* B **74** 155322
[35] Slater J C and Koster G F 1954 *Phys. Rev.* **94** 1498
[36] Saito T and Arakawa Y 2002 *Physica* E **15** 169
[37] Ranjan V, Allan G, Priester C and Delerue C 2003 *Phys. Rev.* B **68** 115305
[38] Schulz S, Schumacher S and Czycholl G 2006 *Phys. Rev.* B **73** 245327
[39] Mourad D, Barthel S and Czycholl G 2010 *Phys. Rev.* B **81** 165316
[40] Wang L W and Zunger A 1994 *J. Chem. Phys.* **100** 2394
[41] Heyd J, Scuseria G E and Ernzerhof M 2003 *J. Chem. Phys.* **118** 8207
[42] Heyd J, Scuseria G E and Ernzerhof M 2006 *J. Chem. Phys.* **124** 219906
[43] Hedin L 1965 *Phys. Rev.* **139** A796
[44] Städele M, Majewski J A, Vogl P and Görling A 1997 *Phys. Rev. Lett.* **79** 2089
[45] Rinke P, Qteish A, Neugebauer J, Freysoldt C and Scheffler M 2005 *New J. Phys.* **7** 126
[46] Rinke P, Qteish A, Neugebauer J and Scheffler M 2008 *Phys. Status Solidi* b **245** 929
[47] Yan Q, Rinke P, Scheffler M and Van de Walle C G 2009 *Appl. Phys. Lett.* **95** 121111
[48] Hybertsen M S and Louie S G 1986 *Phys. Rev.* B **34** 5390
[49] Aulbur W G, Jönsson L and Wilkins J W 2000 *Solid State Phys.* **54** 1
[50] Onida G, Reining L and Rubio A 2002 *Rev. Mod. Phys.* **74** 601
[51] Kümmel S and Kronik L 2008 *Rev. Mod. Phys.* **80** 3
[52] Fuchs F, Furthmüller J, Bechstedt F, Shishkin M and Kresse G 2007 *Phys. Rev.* B **76** 115109
[53] Jiang H, Gomez-Abal R, Rinke P and Scheffler M 2009 *Phys. Rev. Lett.* **102** 126403
[54] Bechstedt F, Fuchs F and Kresse G 2009 *Phys. Status Solidi* b **246** 1877
[55] Janotti A and Van de Walle C G 2007 *Phys. Rev.* B **75** 121201
[56] Qteish A, Al Sharif A I, Fuchs M, Scheffler M, Boeck S and Neugebauer J 2005 *Phys. Rev.* B **72** 155317
[57] Rinke P, Qteish A, Winkelnkemper M, Bimberg D, Neugebauer J and Scheffler M 2006 *Appl. Phys. Lett.* **89** 161919
[58] Qteish A, Rinke P, Neugebauer J and Scheffler M 2006 *Phys. Rev.* B **74** 245208
[59] Davydov V Y *et al* 2002 *Phys. Status Solidi* b **229** R1
[60] Wu J, Walukiewicz W, Yu K M, Ager III J W, Haller E E, Lu H, Schaff W, Saiton Y and Nanishi Y 2002 *Appl. Phys. Lett.* **80** 3967
[61] Nanishi Y, Saito Y and Yamaguchi T 2003 *Japan. J. Appl. Phys.* **42** 2549
[62] Sher A, Schilfgaarde M van, Berding M A, Krishnamurthy S and Chen A-B 1999 *MRS Internet J. Nitride Semicond. Res.* **4S1** G5.1
[63] Bechstedt F and Furthmüller J 2002 *J. Cryst. Growth* **246** 315
[64] Leeuwen R V 2004 *Phys. Rev.* B **69** 115110
[65] Cardona M 2006 *Sci. Technol. Adv. Mater.* **7** 60
[66] Marini A 2008 *Phys. Rev. Lett.* **101** 106405
[67] Kioupakis E, Rinke P, Schleife A, Bechstedt F and Van de Walle C G 2010 *Phys. Rev.* B **81** 241201
[68] Schindlmayr A and Godby R W 1998 *Phys. Rev. Lett.* **80** 1702
[69] Bruneval F, Sottile F, Olevano V, Del Sole R and Reining L 2005 *Phys. Rev. Lett.* **94** 186402
[70] Fleszar A and Hanke W 2005 *Phys. Rev.* B **71** 045207
[71] Shishkin M, Marsman M and Kresse G 2007 *Phys. Rev. Lett.* **99** 246403
[72] Morris A J, Stankovski M, Delaney K T, Rinke P, García-González P and Godby R W 2007 *Phys. Rev.* B **76** 155106
[73] Schleife A, Fuchs F, Rödl C, Furthmüller J and Bechstedt F 2009 *Phys. Status Solidi* B **246** 2150
[74] http://www.sphinxlib.de
[75] Rojas H N, Godby R W and Needs R J 1995 *Phys. Rev. Lett.* **74** 1827
[76] Rieger M M, Steinbeck L, White I, Rojas H and Godby R 1999 *Comput. Phys. Commun.* **117** 211
[77] Steinbeck L, Rubio A, Reining L, Torrent M, White I and Godby R 2000 *Comput. Phys. Commun.* **125** 105
[78] Freysoldt C, Eggert P, Rinke P, Schindlmayr A, Godby R W and Scheffler M 2007 *Comput. Phys. Commun.* **176** 1
[79] Perdew J and Zunger A 1981 *Phys. Rev.* B **23** 5048
[80] Ceperley D and Alder B 1980 *Phys. Rev. Lett.* **45** 566
[81] Moukara M, Städele M, Majewski J A, Vogl P and Görling A 2000 *J. Phys. Condens. Matter* **12** 6783
[82] Kobayashi M *et al* 2009 *J. Appl. Phys.* **105** 122403
[83] Kobayashi M 2009 private communication
[84] Preston A, Ruck B, Piper L, DeMasi A, Smith K, Schleife A, Fuchs F, Bechstedt F, Chai J and Durbin S 2008 *Phys. Rev.* B **78** 155114
[85] Gallinat C S, Koblmller G, Brown J S, Bernardis S, Speck J S, Chern G D, Readinger E D, Shen H and Wraback M 2006 *Appl. Phys. Lett.* **89** 032109
[86] Madelung O (ed.) 1996 *Semiconductors-Basic Data* 2nd revised edn (Berlin: Springer)
[87] Bir G L and Pikus G E 1974 *Symmetry and Strain Induced Effects in Semiconductors* (New York: Wiley)
[88] Kresse G and Furthmüller J 1996 *Phys. Rev.* B **54** 11169
[89] Yan Q, Rinke P, Scheffler M and Van de Walle C G in preparation
[90] Wright A F 1997 *J. Appl. Phys.* **82** 2833
[91] Chichibu S, Azuhata T, Sota T, Amano H and Akasaki I 1997 *Appl. Phys. Lett.* **70** 2085
[92] Shan W, Hauenstein R J, Fischer A J, Song J J, Perry W G, Bremser M D, Davis R F and Goldenberg B 1996 *Phys. Rev.* B **54** 13460
[93] Yamaguchi A A, Mochizuki Y, Sasaoka C, Kimura A, Nido M and Usui A 1997 *Appl. Phys. Lett.* **71** 374

[94] Gil B and Alemu A 1997 *Phys. Rev.* B **56** 12446
[95] Misra P, Behn U, Brandt O, Grahn H T, Imer B, Nakamura S, DenBaars S P and Speck J S 2006 *Appl. Phys. Lett.* **88** 161920
[96] Peng H Y, McCluskey M D, Gupta Y M, Kneissl M and Johnson N M 2005 *Phys. Rev.* B **71** 115207
[97] Ishii R, Kaneta A, Funato M, Kawakami Y and Yamaguchi A A 2010 *Phys. Rev.* B **81** 155202
[98] Gil B, Moret M, Briot O, Ruffenach S, Giesen C, Heuken M, Rushworth S, Leese T and Succi M 2009 *J. Cryst. Growth* **311** 2798
[99] Langer D W and Euwema R N 1970 *Phys. Rev.* B **2** 4005
[100] Wrzesinski J and Frohlich D 1997 *Phys. Rev.* B **56** 13087